The wood strapping was also seiected to limit the restraint on the hoop strain resulting from the pressurization of the pipe. The difference in stiffness between wood and steel provide this flexibility. If the pipe was restrained from deforming radially, the hoop stress would be decreased and the fatigue life increased from what would be expected from in-service pipelines. Strain gages were placed within both restrained and unrestrained regions of the pipe to verify that hoop strains were not reduced.

3.6 SPECIMEN PRESSURIZATION

3.6.1 Hydraulic System

An MTS hydraulic system was used for fatigue testing the specimens. The hydraulic pump is capable of 40 gallons/minute delivered at a pressure of 3000 psi. The hydraulic oil flow rate during testing was lower than 40 gpm due to losses associated with hoses and valves. The hydraulic control unit used was configured with pressure control based on feedback from a pressure transducer on the specimens. The control unit supplies pressure to test-specimens with a volume booster. The volume booster consisted of a hydraulic ram configured with a chamber surrounding the exposed shaft. The chamber was connected to a test specimen. The purpose of the volume booster was to transfer pressure from oil to water. The volume booster was capable of over six gallons of volume change. This represented the maximum volume change that can be experienced by any specimen. The flexible behavior of the dents in the specimens during cycling requires higher volume changes to obtain desired pressures as compared to pipes without damage. The lengths and number of dents allowed per specimen were controlled by the maximum volume change. For this reason, larger diameter pipe specimens were shorter in length, in addition to facilitating handling. Pressure histories were supplied to the hydraulic control unit via a PC-based computer system.

3.6.2 Pressure Histories

To better represent stress conditions indicative for dents in in-service pipelines, a variable pressures profile was used. Normally distributed pressure range histograms, with eight to ten different pressure ranges, were used, as shown in Figs. 3-19 and 3-20. This provided both small and large pressure fluctuations with a mean pressure range of approximately 40 percent of the maximum operating stress of the pipe.

Two types of pressure histories were used for the different pipe specimens. The first history used had a base pressure of 100 psi that is the low peak for every cycle (see Fig. 3-21). The high peaks were of different magnitude randomly distributed. This type of history was used for Specimens 1, 2, 3, 4, 5, and 8.

The second type of history was later developed that used a high base pressure (see Fig. 3-22). The pressures for this type were determined based on hoop stress values. The high base was set to be 60% of the yield pressure. The lower peaks range from 10% to 55% of the yield pressure. The high base pressure was picked because it better simulates pressures in an actual pipe. Two of the 100 cycles in the history range from 10% to 70% of the yield pressure. This history type was picked to achieve a standard history for all pipe sizes such that all specimens have similar profiles in terms of stress.

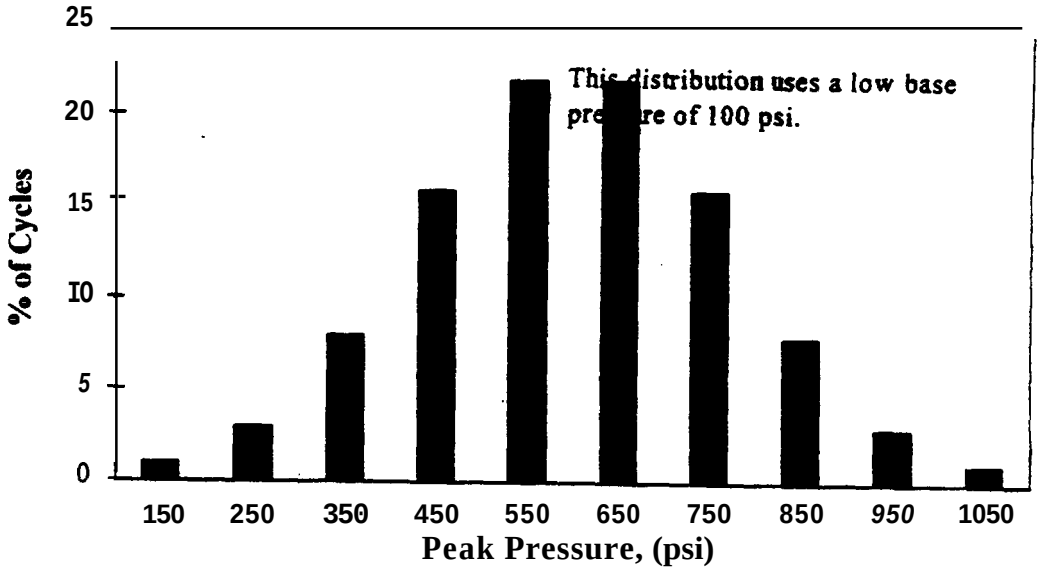

Figure 3-19: Pressure *range* histogram for Specimens 1 & 2 (*high* peaks).

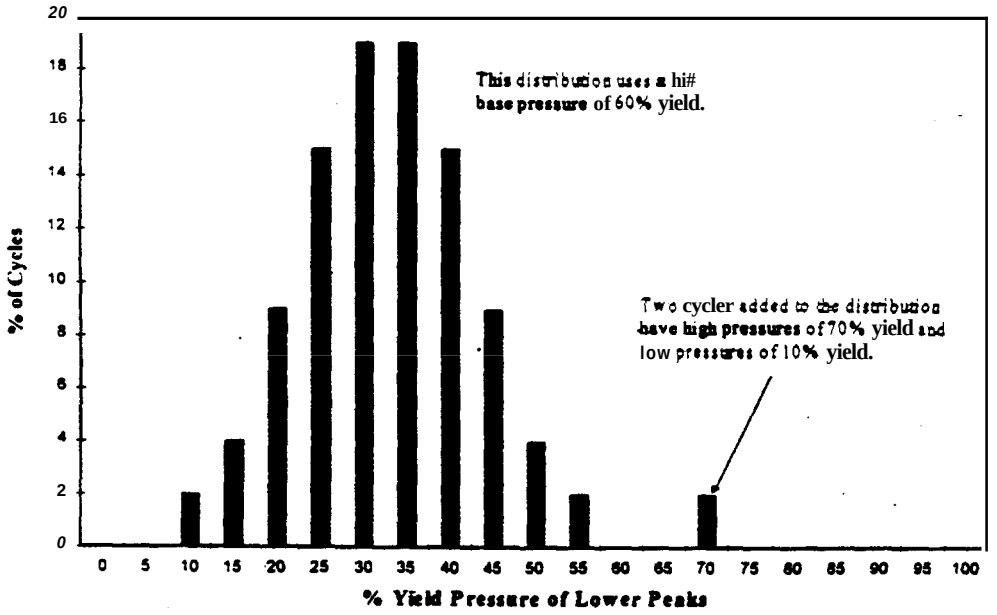

Figure 3-20: Pressure range histogram for Specimens 5, 6, 9 - 15 (low peaks).

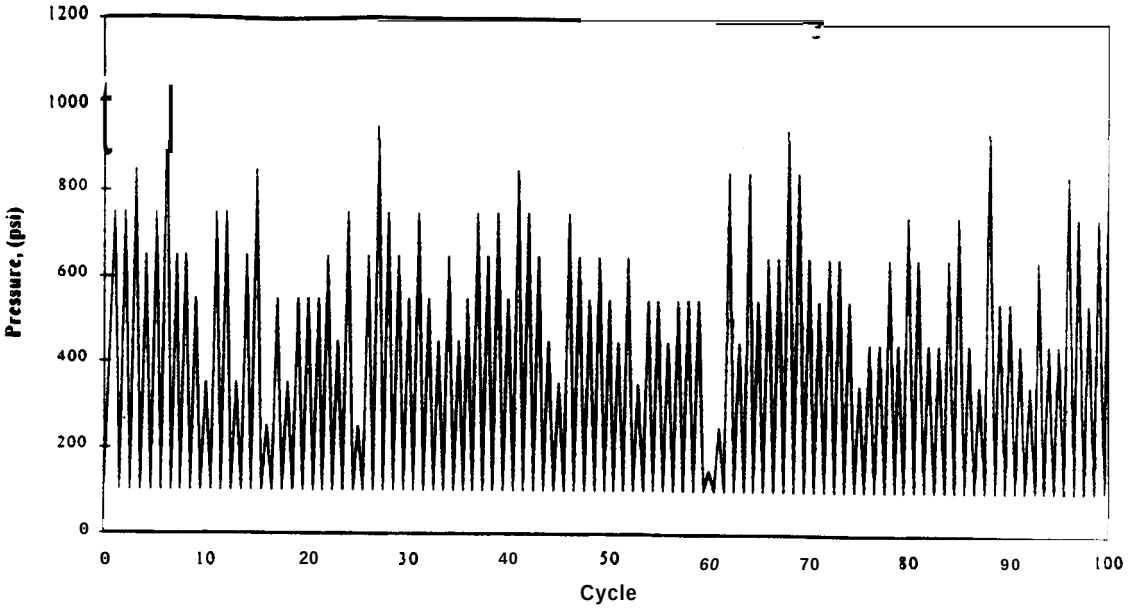

Figure 3-21: Pressure profile for Specimens 1 & 2.

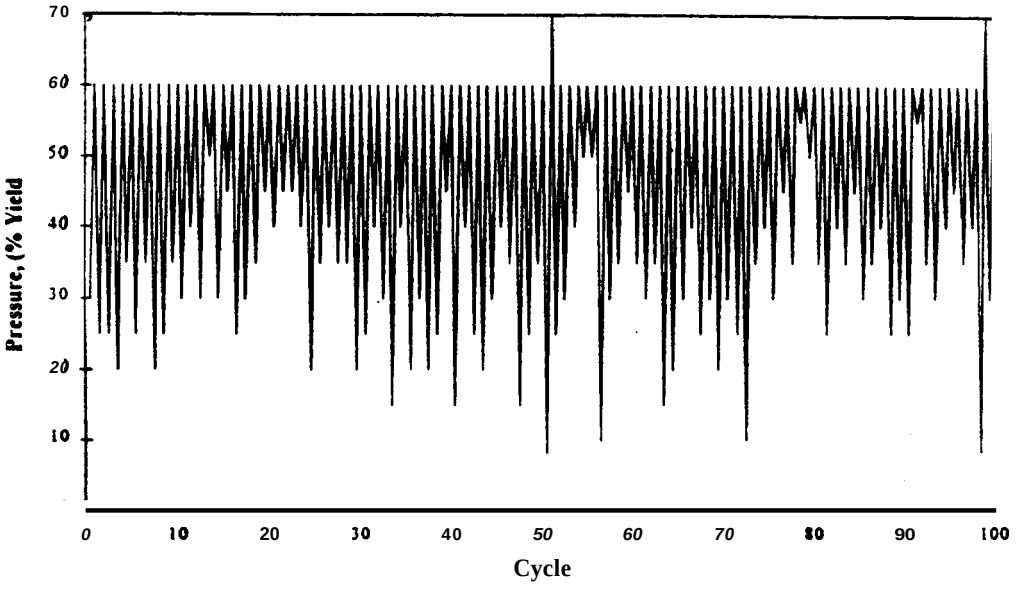

Figure 3-22: Pressure profile for Specimens 5, 6, 9 - 15.

As illustrated in Figs. 3-21 and 3-22, the pressure ranges in the spectrum were randomly ordered in a 100-cycle interval. This interval was then continuously repeated throughout the duration of fatigue testing. An initial estimation for the cycle times was made for each pressure history. A trapezoidal profile is used in the PC-based system to insure that cycle peaks are reached. If the history would not reach its peaks, the cycle times in it would be increased. The times would be decreased if a history easily reached its peaks to decrease overall cycling time. Table 3-4 summarizes the pressure parameters used for each specimen.

Table 3-4: Specimen pressure summaries.

Specimen No.	Base Press. (psi)	P_{min} (psi)	P_{max} (psi)	Effective ΔP (psi)
1	100	100	1050	553
2	100	100	1050	553
3	100	100	1200	721
4	100	100	800	435
5	813	100	948	434
6	720	100	840	383
7	100	100	800	435
8	100	100	800	435
9	536	89	626	285
10	536	89	626	285
11	536	89	626	285
12	536	89	626	285
13	536	89	626	285
14	447	74	521	226
15	447	74	521	226

3.7 FATIGUE TEST PROCEDURES

The general procedure for testing each pipe specimen involves denting, test preparation, static pressurization, fatigue cycling, crack repair, and proof test pressurization. Test preparation involves restraining dents, putting on instrumentation, and filling the pipes with a water-antifreeze mixture. The straps were used for all restrained dents. A section of scrap pipe transfers the load from the straps to the indenter to restrain the dents. The number of straps per dent ranges from four to six depending on dent type and D/t.

The instrumentation included a pressure transducer and a load cell. The transducer sends a feedback signal to the MTS hydraulic system which controls pressure. The load cell was used to record the force required to restrain dents. It is connected between the indenter restraint and the pipe section supplying the force from the straps. Two 1/4 NPT fittings was tapped into one endcap to allow the pipe to be filled. One hole was for draining, and the other was an air vent. The pipes were filled with a water/antifreeze mixture to prevent corrosion of the hydraulic ram used to supply pressure.

Before cycling, static pressurization was performed to obtain dent rebound and restraint load data as a function of pressure. Measurements were taken at several pressure levels up to the maximum pressure used during cycling. Final measurements were taken with zero pressure prior to fatigue cycling.

Cycling was started after the initial static pressurization. A computer generated profile history of 100 cycles is used to cycle the pressure. The pressure history is repeated continuously until leakage occurred. The MTS hydraulic system has limit detectors that will stop the cycling if the pressure gets too low or high. This usually did not stop cycling due to leakage since cracks may only leak at high pressure. Thus, the cyclic testing was checked periodically.

Failure of a dent was defined as the development of a thru-thickness crack. Such a crack was detected by visually detecting the leaking water or by the drop in pressure and triggering of

electronic interlocks. This corresponds to the development of a semi-elliptical, thru-thickness crack. Figure 3-23 shows an example of a leaking fatigue crack in a restrained dent (Type A) on Specimen 4. This crack initiated in the periphery of the dent and was not in the machined notch of this dent type.

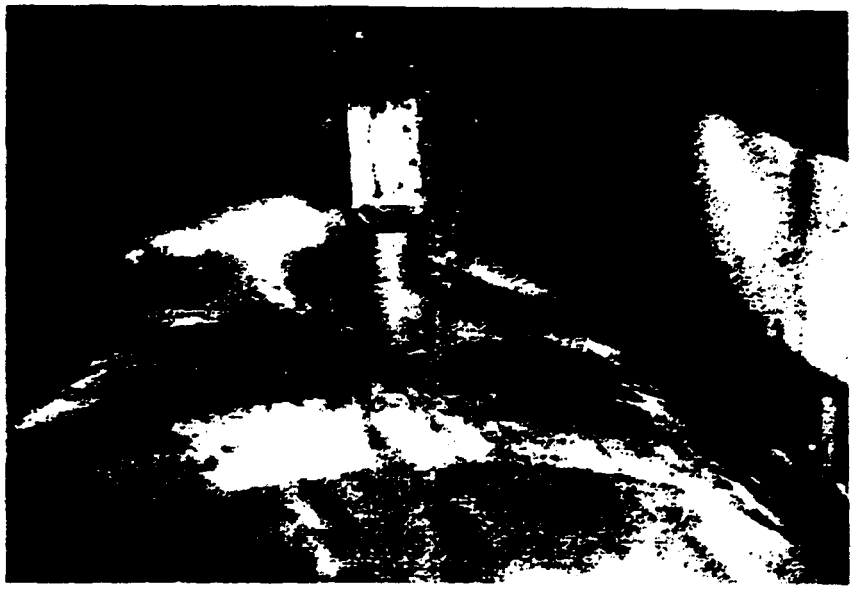

Figure 3-23: View of a leaking fatigue crack in a restrained dent.

Once leaks form, the pressure cycling was stopped and the specimen was drained partially so the water did not act as a heat sink during welding and heat treatment. After the repair, the specimen was filled and cycling continued. Two or three pipe specimens were readied for testing such that a specimen was always available for testing. When one specimen leaked, another specimen could be cycling while the cracked specimen was waiting for repair.

Once cycling was completed, the specimens underwent a high pressure proof test. Specimens were slowly pressurized to 77% of the yield pressure to check for leaks. Specimens were kept at the high pressure for at least 15 minutes. After all parts of testing were completed, dents were cut out of the pipe to be kept for further evaluation. In addition, a section of pipe, located away from any dented region, was removed so that tension coupons could be machined and tested to determine strength properties of each specimen (see Sec. 3.9.7).

3.8 FATIGUE CRACK REPAIR PROCEDURE

Several methods were employed to repair or remove fatigue cracks that propagated to failure so that testing could continue on the remaining dents in a specimen. For the Type A dents, the initial repair was to gouge and weld the *damaged* region. A plasma air-arc torch was used since this equipment results in a relatively clean *gouge* that provides the operator with a clear view of the crack. The gouging was to Within 1/16 in. of the inside wall Surface to allow for the deposition of weld metal without blow-through. Figure 3-24 shows a crack repair gouge prior to welding.

Figure 3-24: Crack *repair* gouge prior to welding.

The welding was performed using the shielded metal arc welding process. Both air-hammer peening of the weld *toes* and grinding of the weld profile was used to improve the fatigue performance of the repair weld. Figure 3-25 shows a completed, multi-pass repair weld with peened weld toe.

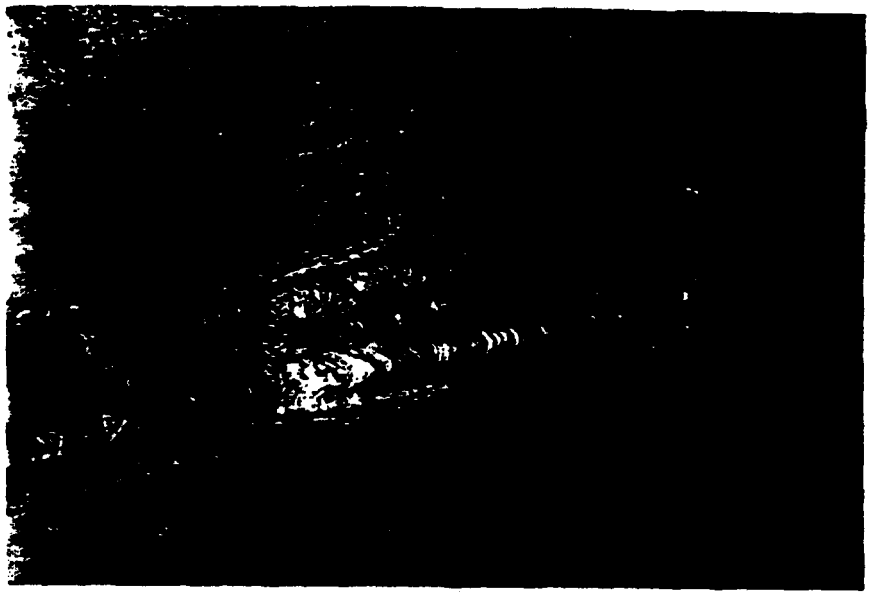

Figure 3-25: Typical multi-pass welded dent *repair* with peened weld toe.

This repair method met with limited *success.* Crack re-initiation would occur if the root pass did not fully penetrate to the inside *surface* of the pipe wall, thus removing the reaming crack after gouging. Too much penetration could result in electrode blow-through. This often resulted in an irregular weld profile inside the pipe and, consequently, difficult to detect. The repair of deep dents often resulted in acute angles for the weld profile and pipe wall. This provided an additional *stress* concentration at the weld toe. Most redevelopment of fatigue cracks occurred on the outside surface at the repair weld toe or between passes. Internal cracks were observed only when the dent region was removed from the specimen after completion of testing.

Periphery cracks (see Figs. 3-52 and *3-59)* that developed at the Type BH and R dents proved to be more difficult to repair since the cracking usually initiated at multiple locations. When the *gouge* and weld repair method was used, it usually resulted in additional cracks forming as the repair weld cooled and tried to contract or quickly developed When cyclic loading resumed.

Another method used to repair the periphery cracks was parallel weld passes over the surface of the pipe wall and relying on the weld penetration to remove the shallower surface cracks. This method was successful as long as the heat from the welding did not expand the cracks, driving them down below the weld penetration where they would reinitiate with continued testing. Figure 3-26 shows a completed dent *repair* using this method.

Figure 3-26: Example of the parallel pass *surf"* weld dent repair method:

A third method used to repair periphery cracks was to heat the cracked region to a temperature sufficient to anneal the steel. This actually would close and seal the shallow surface cracks. Often, the smaller periphery cracks could not be detected until the annealing process was begun and the cracks opened with increasing temperature.

With the limited success of the repair methods, repaired dents that repeatedly redeveloped fatigue cracks were finally removed from the specimen by cutting out the section of the pipe and rewelding the ends together. This repair method also had problems due *to* mismatch in pipe cross sections, especially for the restrained pipes. Some mismatches were off by as much as one wall thickness. Fatigue cracking would initiate on the inside surface.

The repair methods described above are not recommended for use with in-service pipelines. Their use in the present study were implemented only as a means to repair the pipe specimen quickly and allow continued testing of the remaining uncracked dents. With several of the pipe specimens containing eight to ten dents per specimen, the down time for repairs could become significant if the method of sectioning and rewelding was implemented.

3.9 SUMMARY OF RESULTS

In *summary,* the fatigue failures of the dents from the fifteen pipe specimens exhibited two distinct modes of failure:

- single crack development in the contact region of the dent,
- multiple crack development in the dent periphery, outside of the contact region.

The single, elliptical-shaped crack that developed in the mechanically damaged region of a dent is herein referred to as Mode 1. This mode of cracking was found to develop only in the Type A dents. Mode 2 cracking involved multiple crack initiation sites at the longitudinal ends of the dent but outside the contact region. This mode of cracking was found to develop in all types of dents tested but primarily in the Type BH dents and all restrained dents. In addition to the fatigue failures, the force required to form the dents, restraining forces, and dent rebound behavior were also investigated. The experimental results for each pipe specimen are given in detail in the Appendix. The following discussion *summarizes* and highlights some of the more significant test results.

3.9.1 Denting Forces

The maximum actuator forces required to form the dents in the specimens were recorded. With the analysis of this type of data, it may be possible to correlate gouge severity with dent depth. The maximum denting forces required to form the Type A dents are given in Figs. 3-27 and 3-28. Figure 3-27 plots the data by the dent depth (in.) and is differentiated according to the

specimen D/t ratio. As would be expected, the denting force increases with dent depth. Additionally, this relationship is approximately linear for this type of dent. Figure 3-28 plots the same data but differentiated by the dent depth ratio (d/D). While the same general trends are observed. the scatter in the data increases. As seen in both plots, the denting force does not correlate with the D/t ratio. The maximum denting forces required to form the Type BH dents are given in Figs. 3-29 and 3-30. Figure 3-29 plots the data by the dent depth (in.) and is differentiated according to the specimen D/t ratio. The observed behavior for this dent type is similar to the Type A dent but with more scatter. The denting force increases with dent depth and the relationship is approximately linear. Figure 3-30 plots the same data but differentiated by the dent depth ratio (d/D). Figures 3-31 and 3-32 show the denting forces for the Type R dents. Again, these data shown the same trends as the other two dent types. Note the reduced scatter in Fig. 3-31.

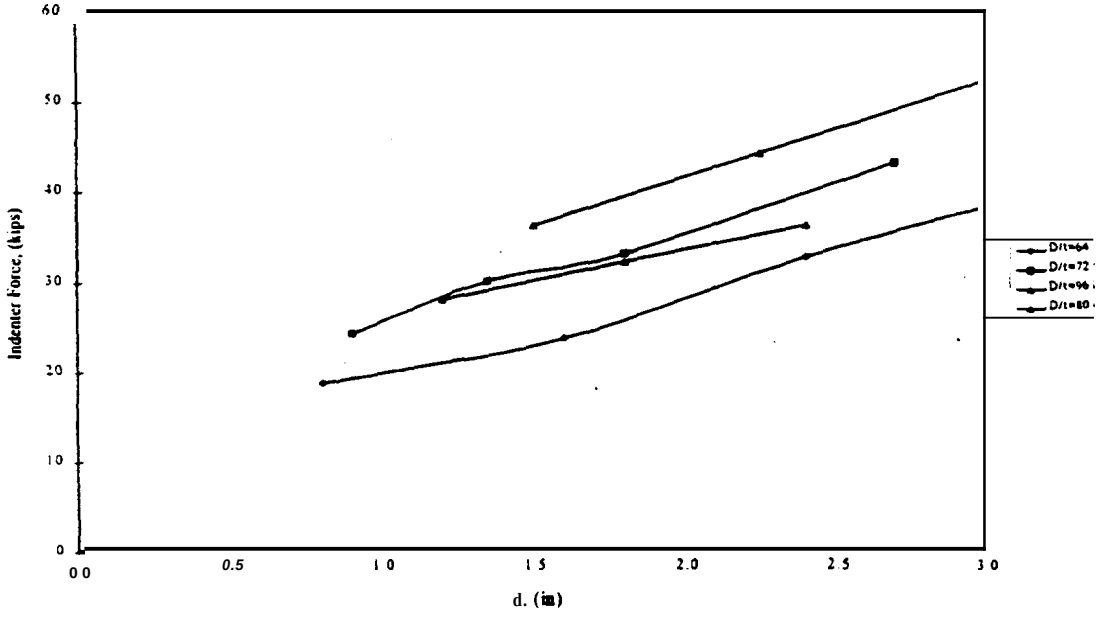

Figure 3-27: Measured denting forces by dent depth for Type A dents.

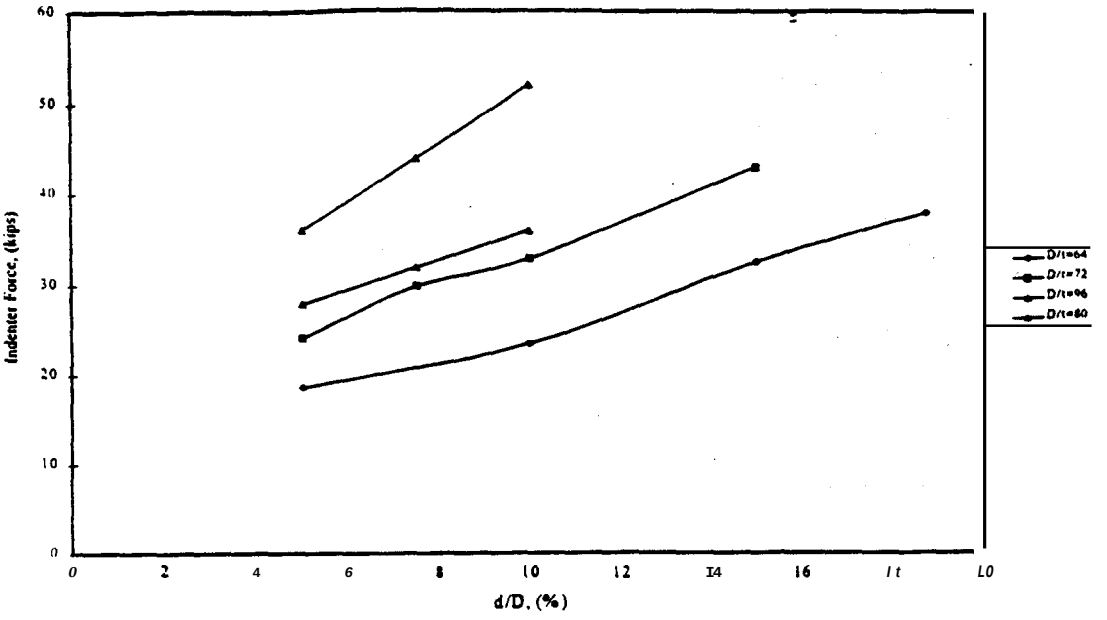

Figure 3-28: Measured dent forces by dent depth ratio for Type A dents.

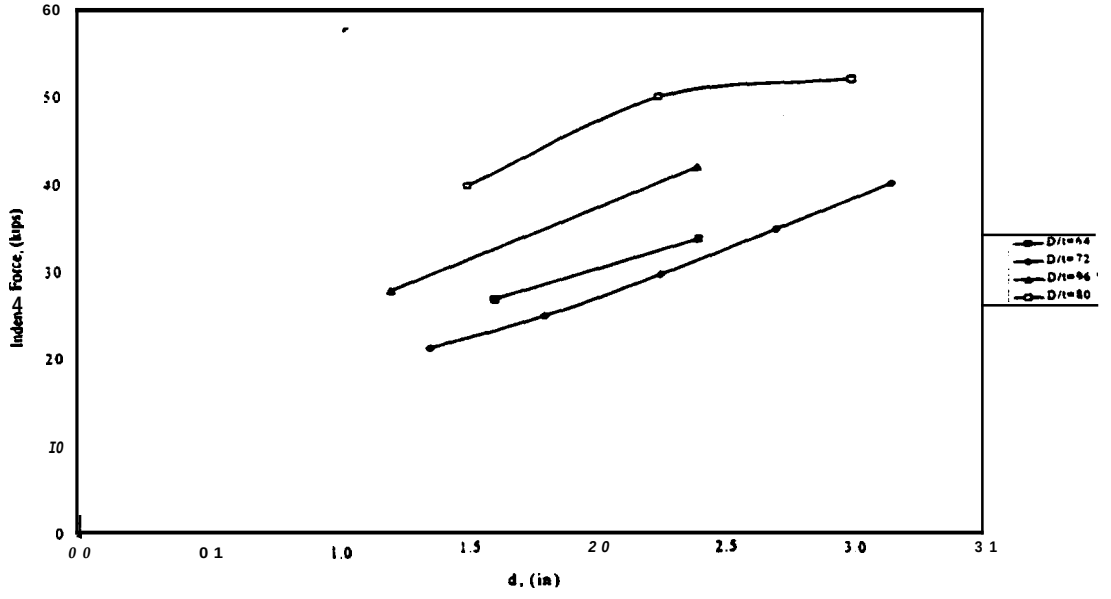

Figure 3-29: Measured denting forces by dent depth for Type BH dents.

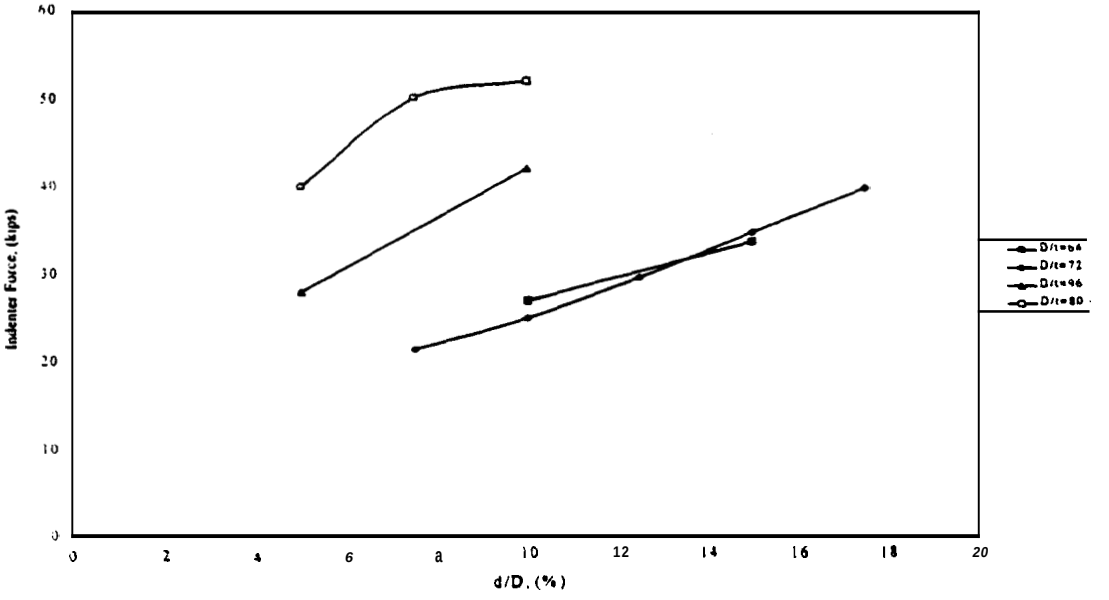

Figure 3-30: Measured denting forces by dent depth ratio for Type BH dent.

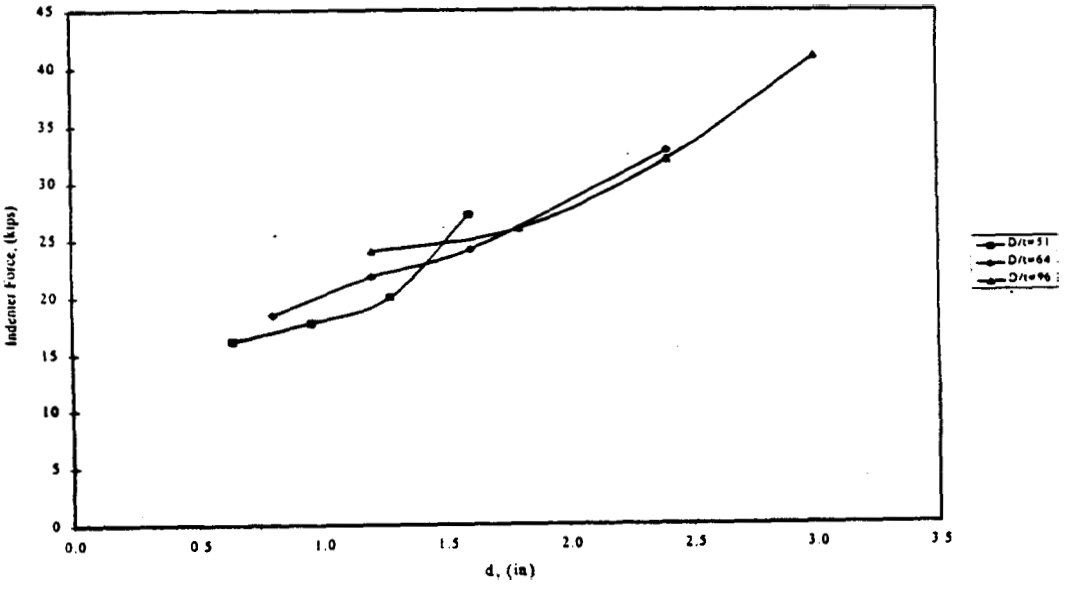

Figure 3-31: Measured denting forces by dent depth for Type R dents.

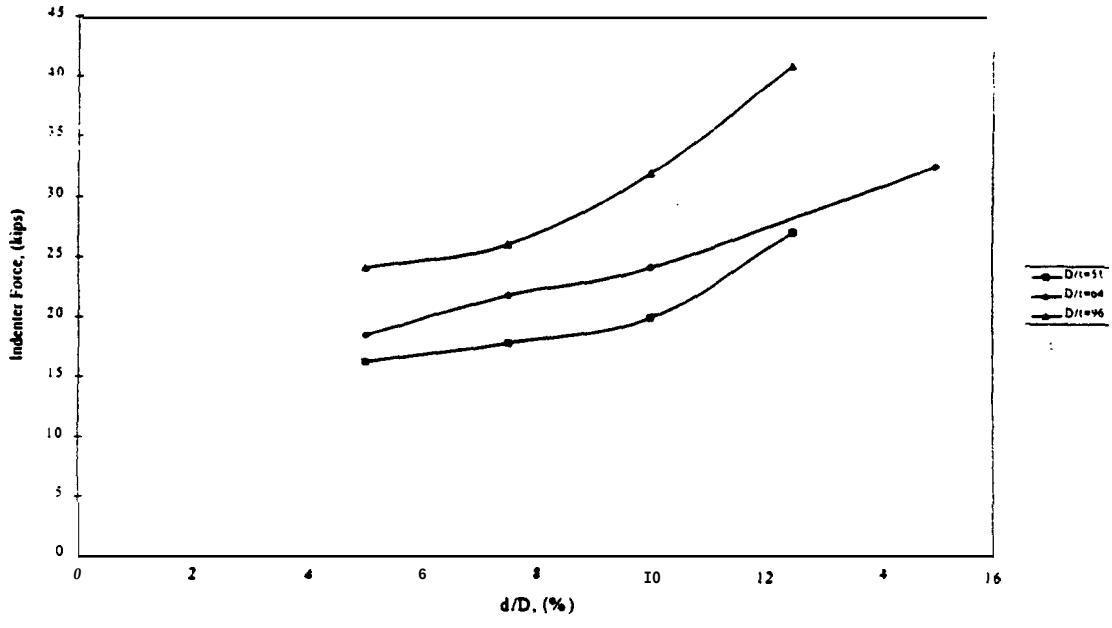

Figure 3-32: Measured denting forces by dent depth ratio for Type R dents.

3.9.2 Restraint Forces

To provide an understanding of restraint forces, a 50 kip load cell was used to measure restraint forces that develop with both the installation of the restraint straps and the pressurization of the pipe. Knowing the magnitude of the restraint forces, the severity of rock dents (Type R) as a function of the rock compressive strength can be estimated. Low strength rocks will degrade as the pipe settles, resulting in a more rounded, less severe dent profile. Measurements were recorded for all three dent types on various pipe sizes. Figure 3-33 shows the load cell and restraint assembly for Pipe Specimen 7 with a Type BH dent.

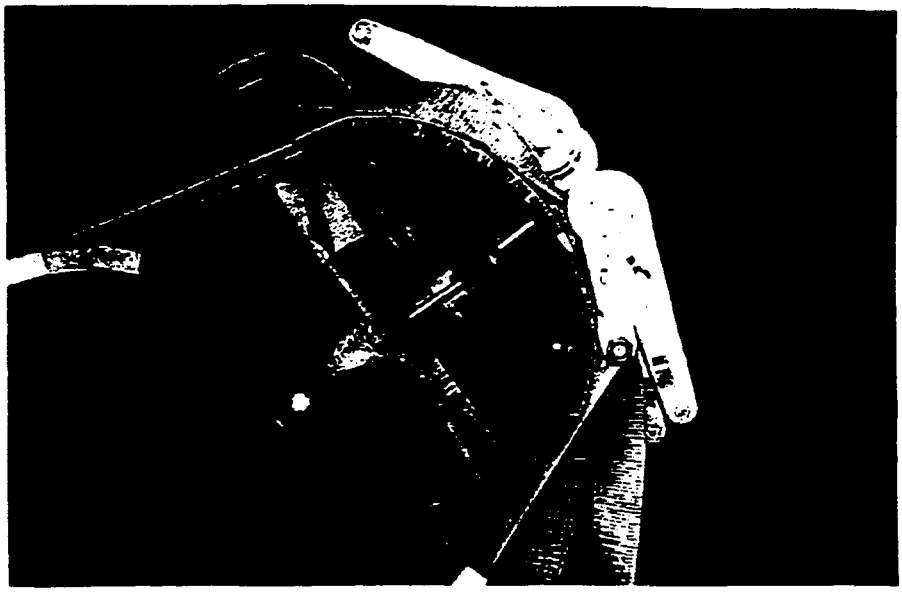

Figure 3-33: View of load cell arrangement with restrained backhoe tooth, Specimen 7.

Rock dents were restrained in similar fashion as the other restrained dents (see Fig. 3-34). The same rock that was used to form the dent was used as the restraint so that the dent profile matched that of the rock. A load cell was placed under several of the restrained rocks to determine restraint forces under both static and dynamic load conditions.

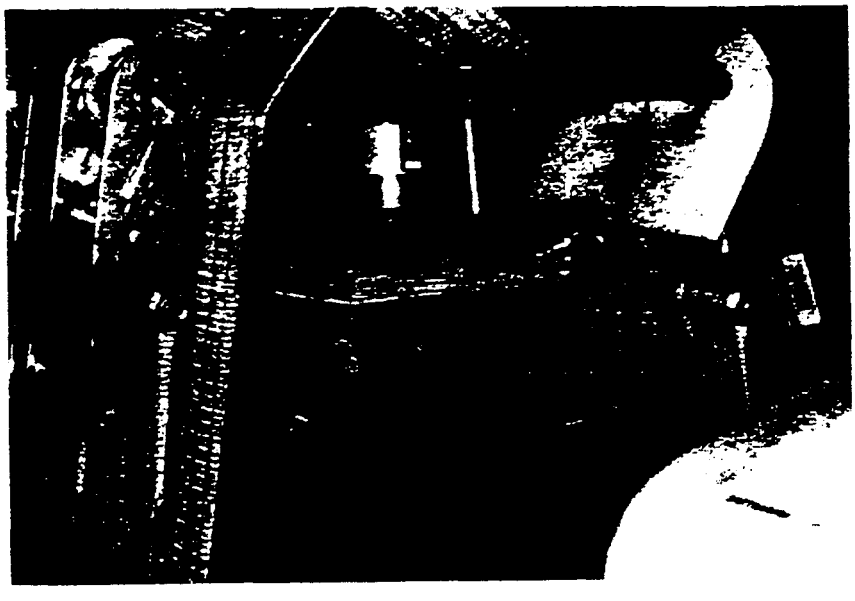

Figure 3-34: Restrained rock dent (Dent G) with load cell, Specimen 3.

Figure 3-35 shows the measured restraint forces for the Type A dent as a function of the hoop stress based on the internal pipe pressure. As expected, the restraint force increases with increasing pressure. The three data sets for the 10 percent dent depth show that the restraint force increases as the D/t ratio increases.

As previously mentioned, several Type BH dents were restrained on three of the specimens tested. As shown in Fig. 3-36, the data does not exhibit any pronounced trend with respect to the dent depth. Regard to the D/t ratio, the smaller diameter specimen ($Dlr = 34$) showed a smaller change in restraint force with internal pressure than the larger diameter specimen ($Dlr = 72$). This may be due to the increased stiffness of the Type BH dents in pipes with smaller Dlt.

Figure 3-37 shows the measured restraint forces for two Type R dents in separate pipe specimens. Both dents had initial dent depths of 10 percent. The dent in the larger diameter pipe ($D/t = 96$) exhibited higher and more varied restraint forces, though the initial restraint forces (at zero pressure) was greater.

The significant of the restraint force data is that it shows the magnitude of force required to prevent or minimize the dent rebound. Restraint force approaching 30 kips were observed. If the strength of the object providing the restraint is exceeded by the force, the degree of restraint will be reduced or lost. This will probably change the fatigue behavior of the dent and its mode of failure.

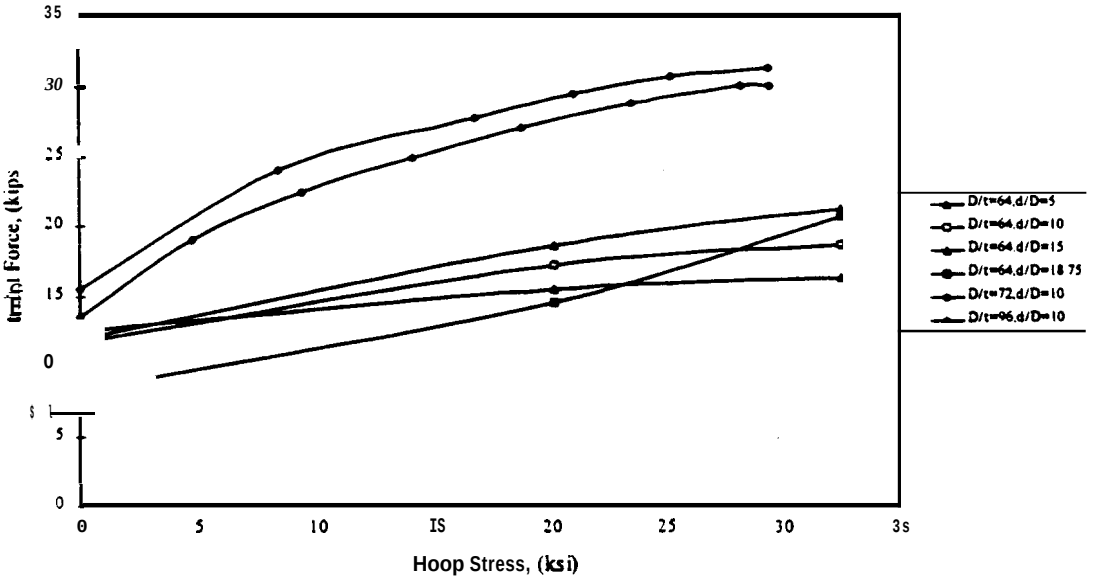

Figure 3-35: Measured restraint forces for Type A dents.

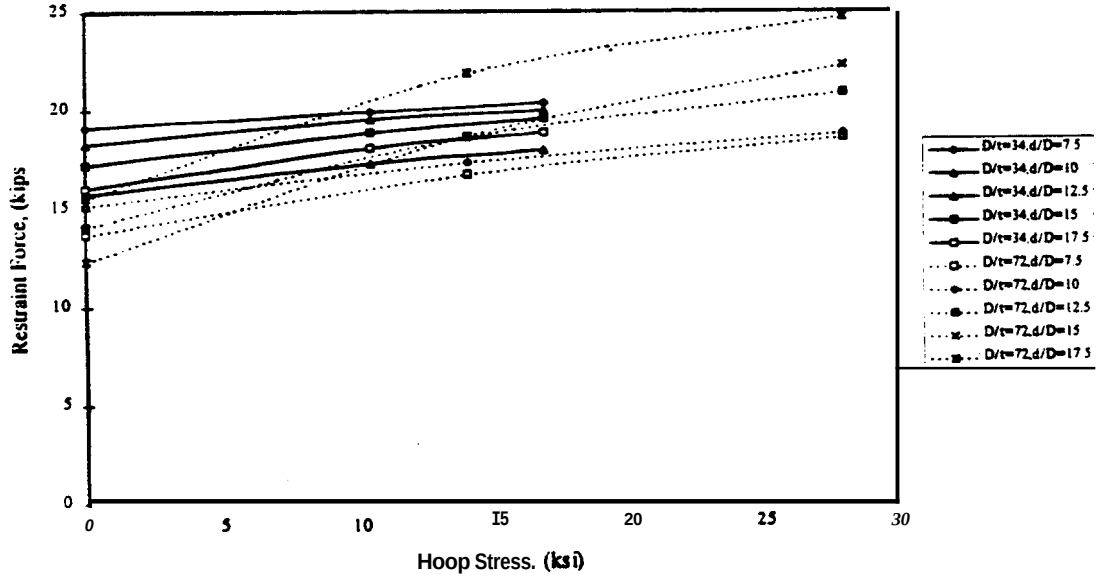

Figure 3-36. Measured **restraint forces for Type BH dents.**

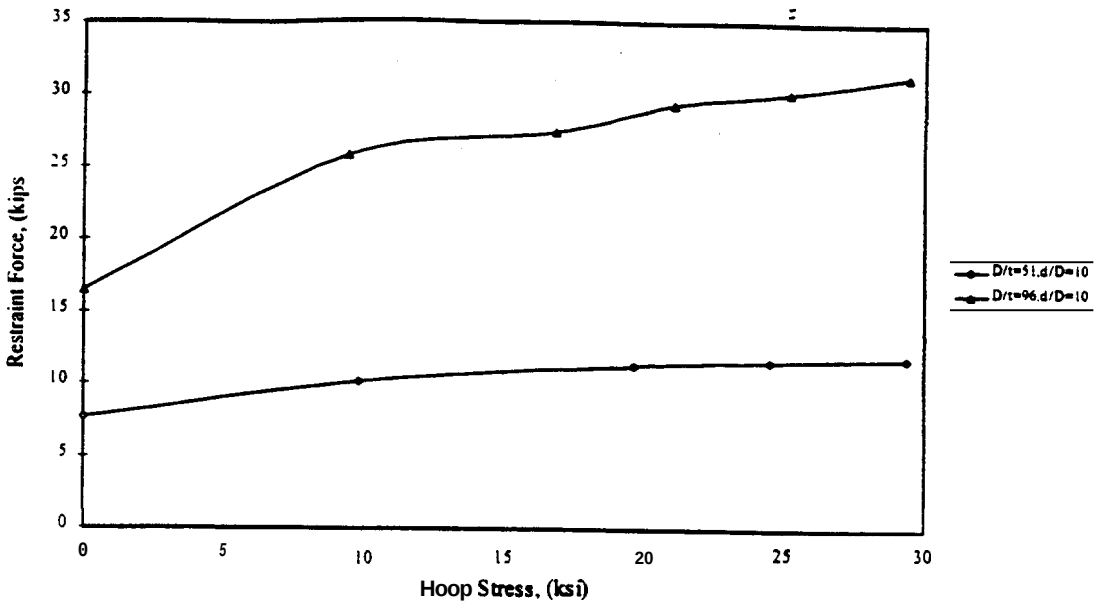

Figure 3-37: Measured restraint forces for **Type** R dents.

3.93 Dent Rebound Behavior

Extensive measurements were taken of dent depths. The general rebound behavior can be classified into three distinct stages:

- initial formation to **maximum** dent depth,
- elastic rebound with indenter removal,
- plastic rebound under pressurization.

The maximum dent depth was prescribed for each dent in terms of percent of the pipe diameter. Dent depth measurements were then taken after the dent rebounded with the removal of the indenter and at different internal pressures. The following discussion summarizes those measurements.

Unrestrained Type A Dents

The dent rebound behavior for the unrestrained Type A dents is illustrated in Figs. 3-38 and 3-39. Figure 3-38 plots the data by the dent depth (in.) and is differentiated according to the specimen *D/t* ratio. The dent depth decreases with increasing internal pressure. With the exception of the 12 in. diameter pipe specimen (*D/t* = 34), the dent depths converge as the pressure increases. Figure 3-39 show the same general trends.

The significance of this data is that the final or residual dent depth is not necessarily an indication of the initial dent depth. For example, a 2.6 in. deep dent in a pipe with a *D/t* of 72 converges to the same depth (0.3 in.) as a 1.2 in. deep dent in a pipe with a *D/t* of 96.

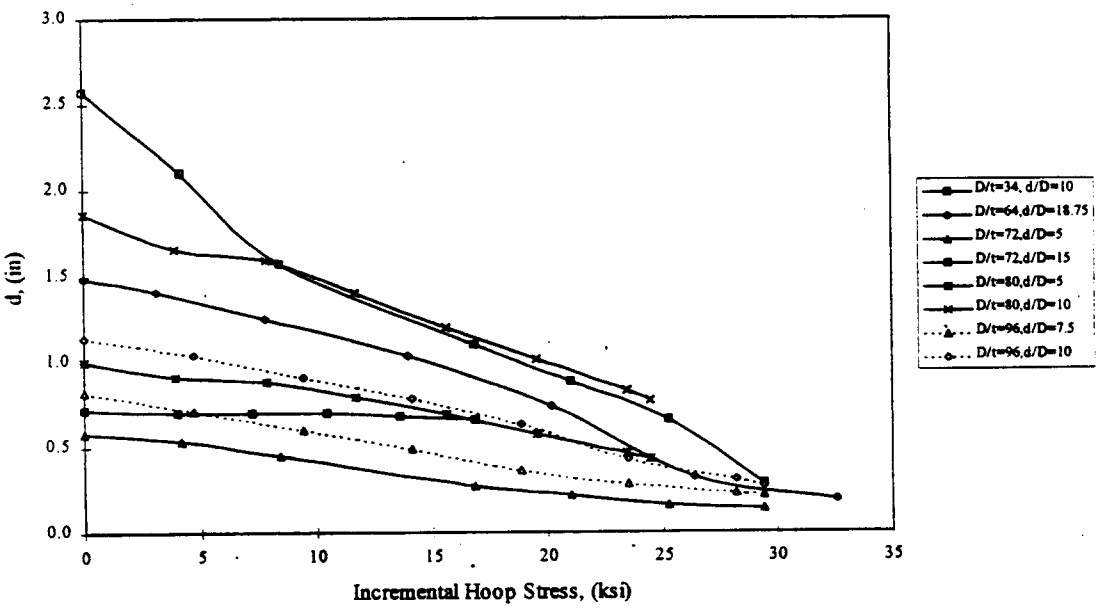

Figure 3-38: Dent Type A rebound behavior in terms of *d*.

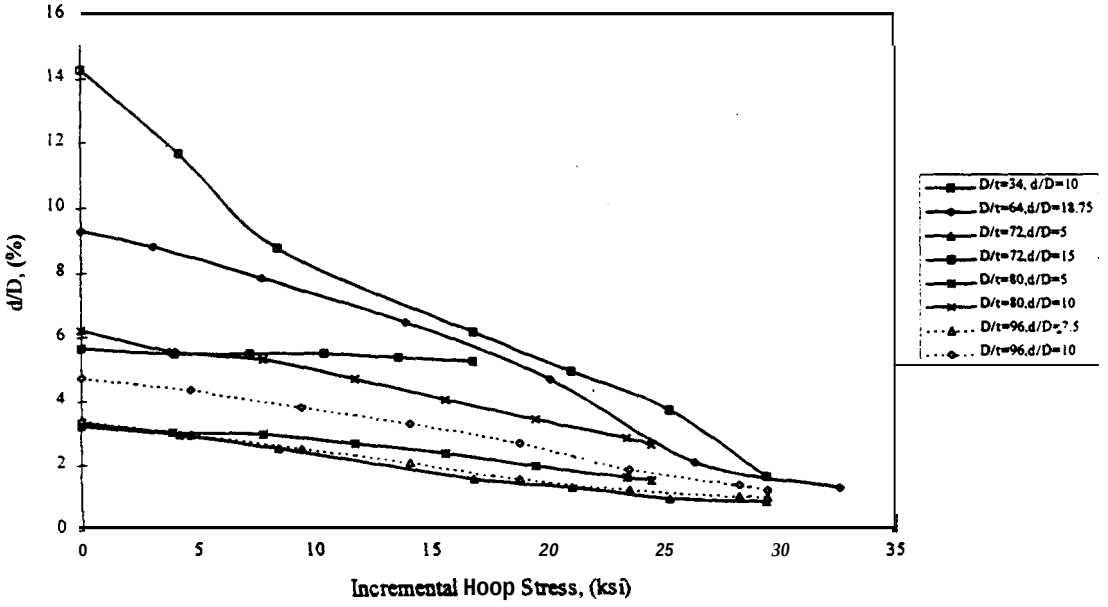

Figure 3-39: Dent Type A rebound behavior in terms *d/D*.

Preliminary results show that the amount of elastic and plastic rebound of a dent is a function of the *D/t* ratio and the pipe diameter. Figure 3-40 shows the measurements for the dent depths of Specimen 6 (*D* = 18 in. and t = 0.25 in.) taken during the initial static test. The unrestrained dents rebounded to depths that are similar in magnitude, although the initial dent depth varied greatly.

As indicated by the plotted depths, the measured depth at the time of inspection/detection does not reveal the denting and rebound history. Dents that have similar depths can have different histories, and, consequently, much different fatigue lives. The severity of this condition increases with increasing pipe diameter. It is anticipated that the dent acceptance criteria will be more restrictive for the larger diameter pipe. However, the fatigue testing of the larger diameter pipe specimens is needed to confirm this.

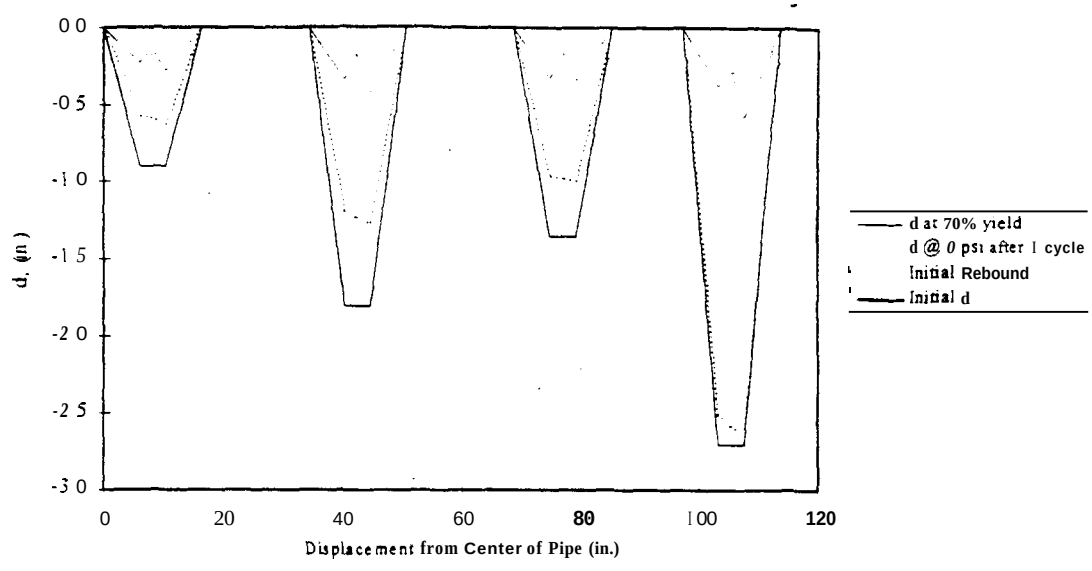

Figure 3-40: Dent depth histories for Specimen *6*.

Another important observation of the rebound behavior of the unrestrained Type **A** dents was the existence of a bulge at the center portion of the contact region of the dent. An example of dent bulging is shown in Fig. 3-41 for dent B **of** Specimen **9** (*D* = 24 in. and *t* = 1/4 in.). The presence of the bulge indicates that the this region of the dent is undergoing a greater degree of stress reversal than regions or dents without bulging. The initial formation of the dent places the contact region in positive curvature (compressive bending stresses on the outside surface). With indenter removal **and** pressurization, a negative curvature develops, placing the outer surface in tension. Therefore, a bulging region **is** more susceptible to fatigue damage **than a** region without the bulge.

The **unrestrained Type A** dents in pipe specimens with diameters of 12 to **24** inches showed bulging. Of interest **was** the lack of bulging in the larger diameter pipes. The unrestrained Type **A** dents in Specimens **12** (*D* = 30 in. and *t* = 3/8 in.) and 14 (*D* = *36* in. and *t* = 3/8 in.) did not develop the bulging rebound behavior. Specimens 9 and 14 **both** have a *Dlt* = 96, but have different rebound characteristics primarily influenced by change in diameter.

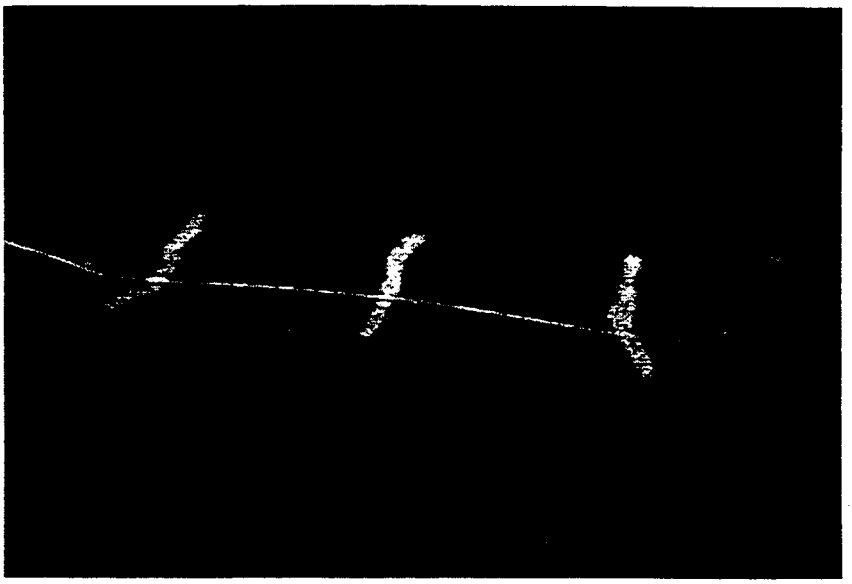

Figure 3-41: Bulging Type **A** dent, Specimen 9.

Type BH Dents

The dent rebound behavior for the unrestrained Type BH dents is illustrated in Figs. **3-42** and **3-43.** Figure **3-42** plots the **data** by the dent depth (in.) and is differentiated according to the specimen D/t ratio. **As** with the Type **A** dents, the dent depth decreases with increasing internal pressure. However, the change in dent depth is not **as** large. Note that the dent depth for the **12** in. diameter pipe specimen **(D/t = 34)** does not significantly change with the change in pressure. Figure **3-43** shows the same general trends.

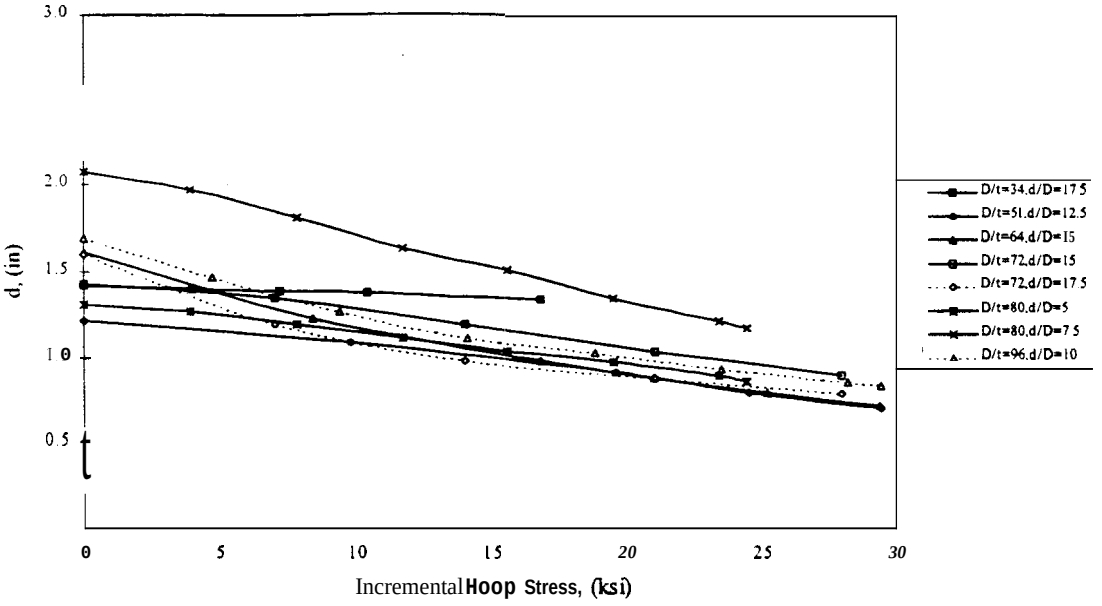

Figure 3-42: Dent Type BH rebound Behavior in terms of *d*.

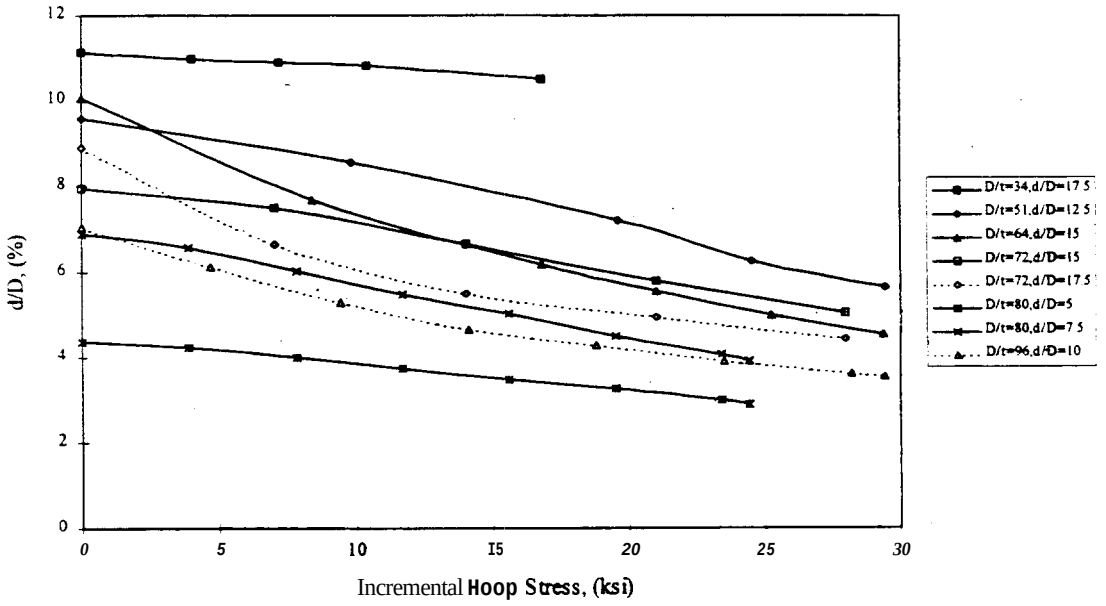

Figure 3-43: Dent Type BH rebound behavior in terms of *d/D*.

3.9.4 Fatigue Behavior of Dents with Mechanical Damage (Type A)

Unrestrained Type A Dents

For the most part, the unrestrained dents with mechanical damage (Type **A)** developed fatigue cracks in the machined notch or scratch at or near the center portion of the dent. Figure 3-44 shows a dent that has developed a fatigue crack along the machined notch (Mode 1). This center region of the dent length was observed to exhibit more elastic rebound or bulging than at the outer extremes of the dent. This is indicated by the dent depth histories plotted in Fig. 3-40. Consequently, the stress concentration factor changes with internal pressure, and fatigue damage accumulation is nonlinear.

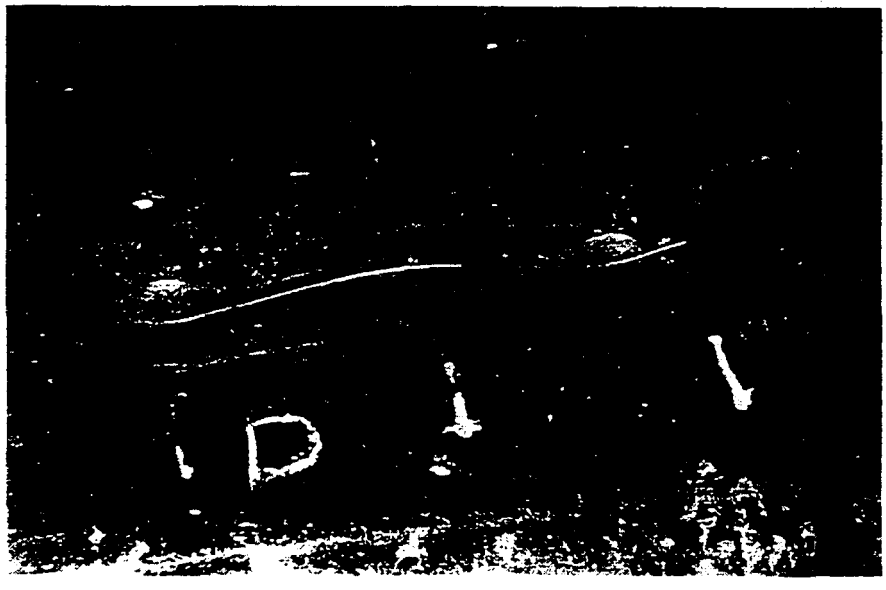

Figure 3-44: Failed Dent D, Specimen **4.** Note bulge at center region of dent.

Upon completion of the specimen fatigue testing, several of the **Type A** dents that had not reached failure were sectioned and broken open to expose any cracking. Figure **3-45** shows a semi-elliptical crack that developed in Dent **A** of Specimen 1. Note that the crack was near thru-thickness at the time cyclic loading was stopped. The fatigue lives of the unrestrained Type **A** dents are summarized in Fig. 3-46.

Figure 3-45: Exposed fatigue crack for Type A dent (from Dent A, Specimen 1).

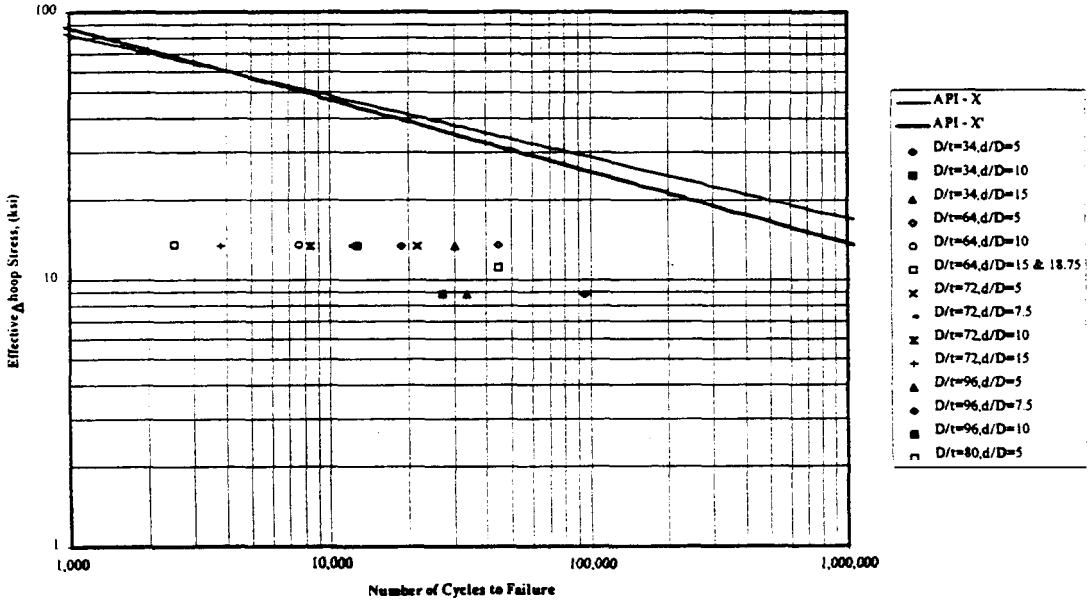

Figure 3-46: S-N plot of fatigue failures for unrestrained Type A dents.

Of interest with the unrestrained Type A dents was the change in fatigue behavior for Mode 1 (contact region cracking) to Mode 2 (periphery cracking) with the larger diameter specimens. As discussed previously in Sec. 3.9.3, these dents exhibited significantly less bulging in the contact region. For Specimen 12 ($D = 30$ in., $t = 3/8$ in.), fatigue cracks only developed in the dent contact region. The shallowest dent depths resulted in the lowest fatigue lives of the three dents tested. For Specimen 14 ($D = 36$ in., $t = 3/8$ in.), the shallowest dent failed first, initiating at the center of the contact region. The two deeper dents developed peripheral cracking, though neither dents developed thru-thickness cracks *after* 100,000 pressure cycles. The deeper dents in the larger diameter specimens have improved fatigue behavior over the shallower dents.

The observed behavior of the unrestrained Type A dents in large diameter pipes suggests a transition in probable failure modes from Mode 1 to 2. This transition is influenced by both diameter and initial dent depth. As both the diameter and initial dent depth increases, the dent stiffness increases, limiting dent rebound. The increase in dent stiffness increases the fatigue performance of the dent contact region by limiting the reversal of the residual Compressive stresses in the contact region.

Restrained Type A Dents

The fatigue life of restrained type A dents is given in Figure 3-47. Fatigue cracks developed in peripheral regions of all failures (Mode 2). The restraint does not allow elastic rebound of the center portion of the dent. This region maintains compressive residual stresses during pressurization unlike the unrestrained dents. The effect of the restraint changes the mode of fatigue failure. The peripheral regions of the dent attempt to rebound around the restraint putting the area in tension. This region does not experience as much plastic strain or deformation as the center of the dent. The flexibility of the center portion of the dent makes the peripheral regions have higher tensile stresses, which influences the fatigue life. Larger dent depths have shorter fatigue lives. This trend applies to all dents tested. The increase in dent depth increases

the flexibility of the restrained portion of the dent which requires the peripheral regions to *carry* additional tensile stresses upon pressurization.

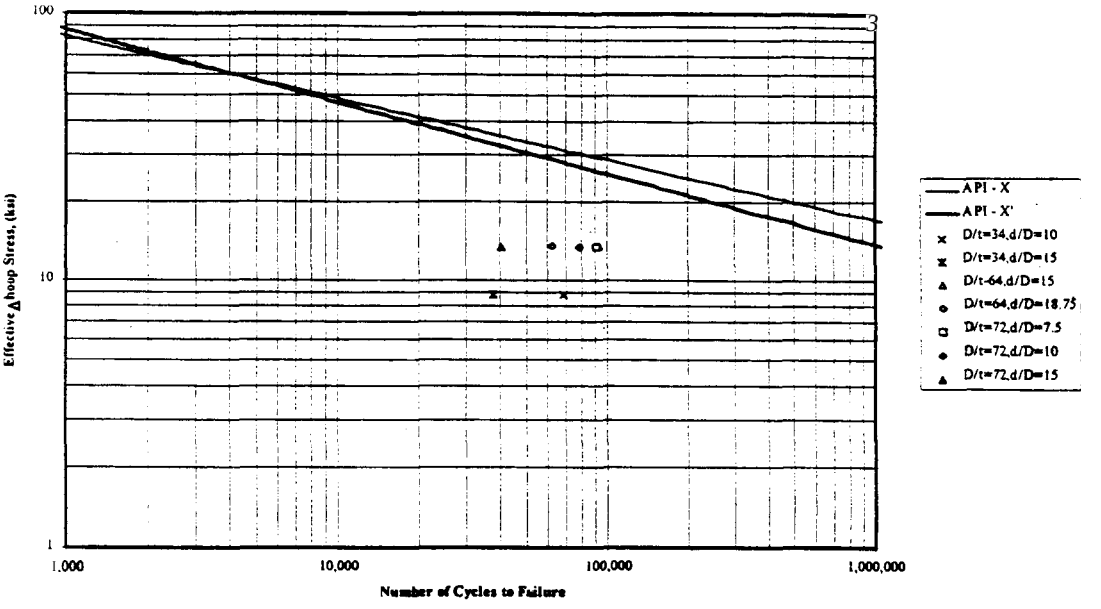

Figure **3-47:** S-N plot of fatigue failures for restrained Type **A** dents.

Effect of Dent Restraint - Type A

The modes of failure of **restrained** and unrestrained **type A** dents are different. Unrestrained dents fail in the center of the dent after the dent experiences elastic rebound which puts this area of the dent in tension. Since restraint does not allow **this** behavior, tensile stresses in the periphery of dents **are increased,** leading to **a** different mode of failure. The different mode significantly increases the fatigue life. Figure 3-48 shows the fatigue lives of restrained and unrestrained dents. When comparing the two dents **with** similar values of *d/D*, the restrained dents have significantly longer fatigue lives.

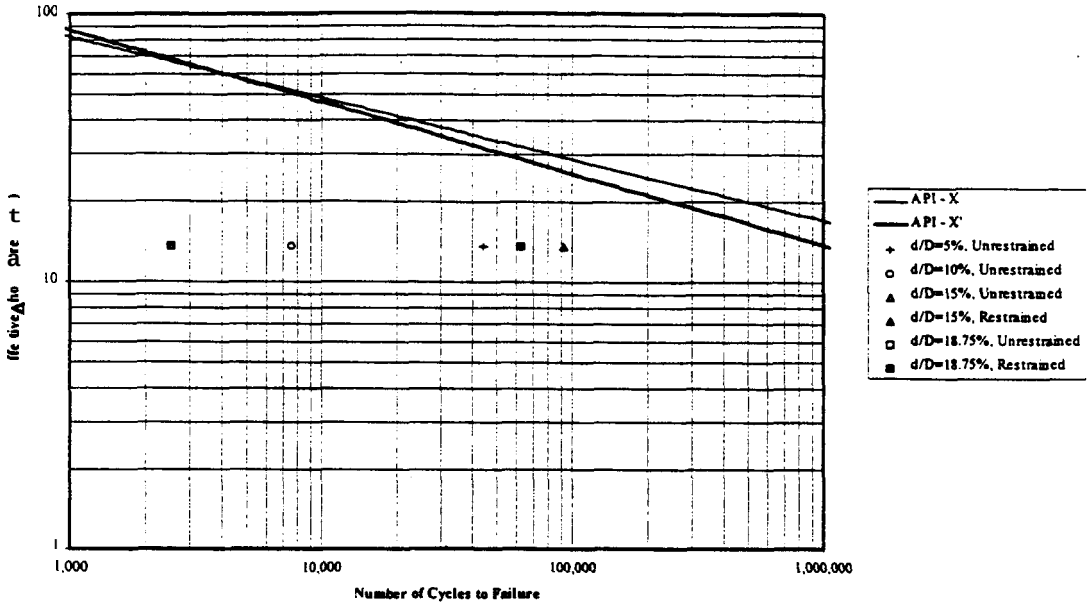

Figure 3-48: S-N plot of fatigue failures for Specimen 4 (Type A).

Summary of Type A Dent Behavior

The experimental results show that dent length influences the fatigue behavior of unrestrained dents when the dent is oriented with the longitudinal axis of the pipe. As the dent length increases, the restraint of the dent trough in the inner portion of the dent length decreases, allowing this portion of the dent to reverse in curvature, or "pop out," thus placing the outer surface of the dent in tension. A more pronounced bulge was often observed for the deeper dents.

3.9.5 Fatigue Behavior of Dents from Backhoe Teeth (Type BH-L and BH-T)

The fatigue testing of dents produced by the backhoe teeth oriented in both the longitudinal and transverse directions did not produce any detectable cracks in the contact region. This was observed for all dent depths and pipe *D/t* ratios when fatigue tested to 100,000 pressure cycles. The lack of failure in these dents can be attributed to two reasons. The gross plasticity

that occurs during denting results in high residual compressive stresses in the region of expected crack growth (see Fig. 3-49). The presence of compressive residual-stresses suppresses crack growth due to the reduction of the stress ratio. Secondly, restraint due to the sharp geometry of the dent cross section prevents significant elastic rebound of the dent. Consequently, the outer surface of the dent trough is not brought back into tension as is the case with other type dents (Type A in this study, for example). Dent bulging cannot occur with this type dent, as shown in Fig. 3-50.

Figure 3-49: Dent F, Specimen 2 showing deformation at contact region.

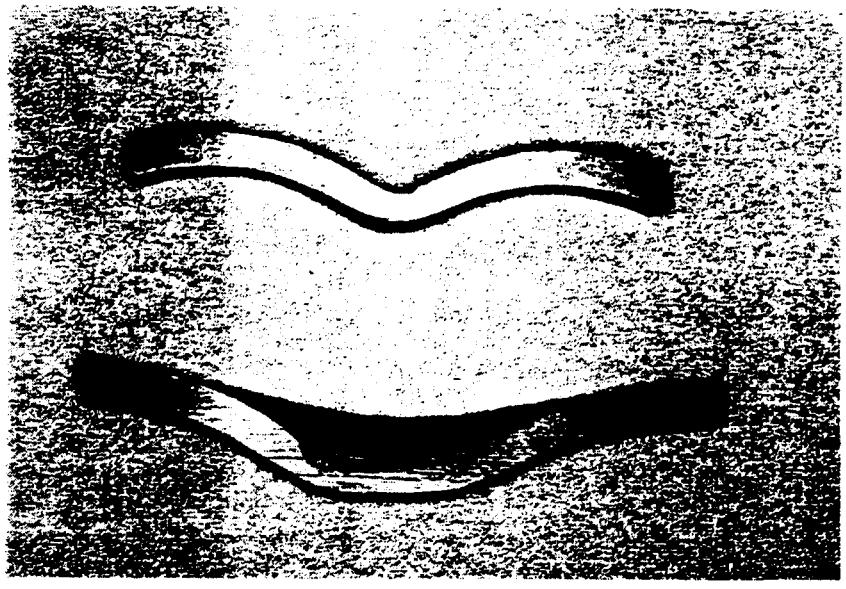

Figure 3-50: Cut cross sections of Dents E (top) and F (bottom), Specimen 2.

All failures of type BH dents were caused by peripheral cracking (Mode 2). Dent types BH-L and BH-T have similar fatigue behavior. Failures of both types have occurred for d/D ratios of ten percent or larger. Figure 3-51 shows type BH-L failures. Type BH-T failures are given in Fig. 3-52. Several Type BH dents were restrained to determine the effect of restraint. Restraint was found to have no significant change in dent behavior for two reasons. First, both cases have the same type of peripheral cracks. Second, unrestrained rebound is not that great as compared to type A dents due to the sharp geometry of the dent.

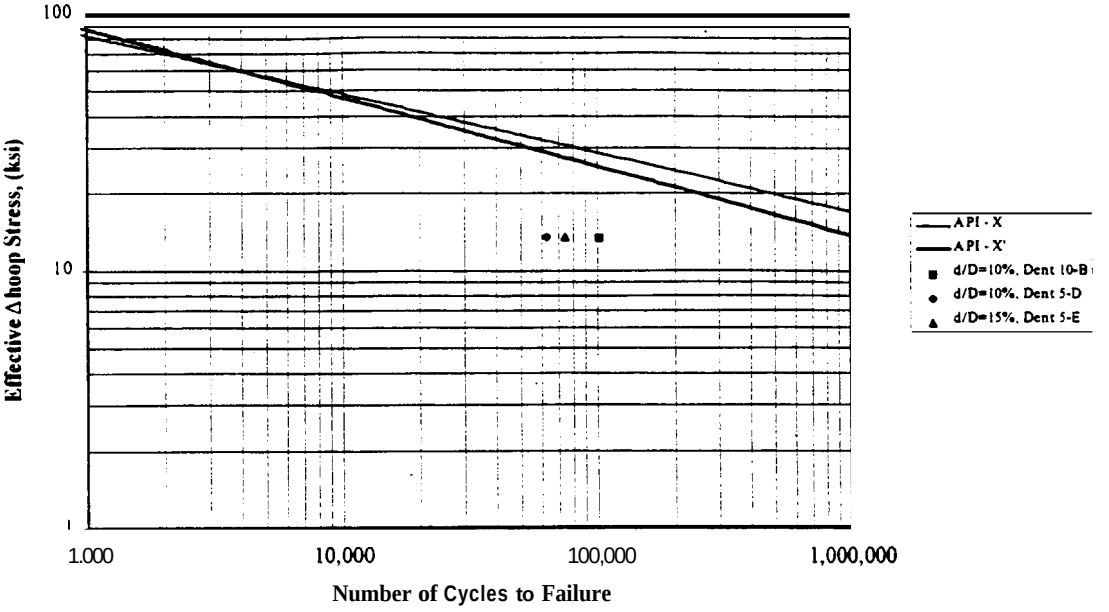

Figure **3-51:** S-N plot of fatigue failures for Type BH-L **dents.**

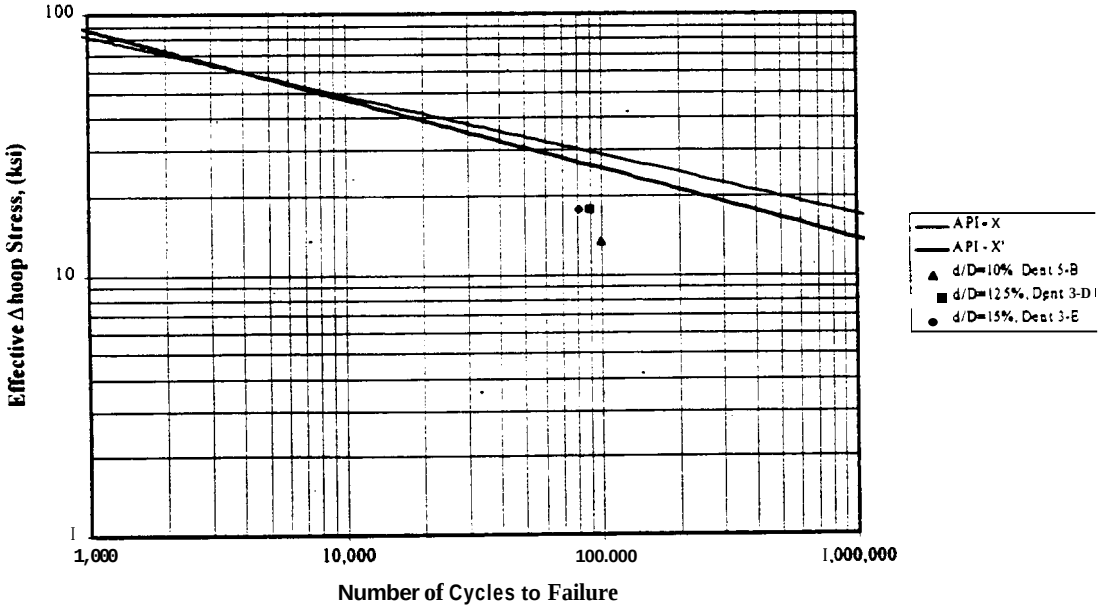

Figure **3-52:** S-N plot of fatigue failures for Type BH-T **dents.**

Fatigue cracks did not develop fiom this type of dent in the 12-inch diameter pipe (D/t = 32). However, the restraint provided by the pipe wall stiffness decreases with increasing pipe diameter. Periphery cracking has been observed for the same type of dent in the larger diameter pipe.

Figure 3-53 shows a periphery crack that developed on the negative curvature dent surface, removed fiom the dent trough. Figure 3-54 shows the cracked region cleaned and removed fiom the dent, while Fig. 3-55 the same crack exposed. Note the multiple crack initiation sites on the wall outer surface (top) that coalesce to form a single semi-elliptical crack that propagates inward. Past research has indicated that this type of cracking is due to the strain-hardening of the steel during denting (Urednicek 1986). However, both finite element analysis and analytical plate bending models do not produce strain levels sufficient for strain-hardening. The severity of a periphery crack is a function of restraint provided by the pipe wall curvature and thickness, as well as pipe diameter. The stress concentrations that form around the dent are similar to those found around a hole.

Figure 3-53: Dye-penetrant inspection of fatigue crack at periphery of Dent F, Specimen 7.

Figure 3-54: Close up view of removed **wall** section containing **cracking,** Dent F, Specimen **7.**

Figure 3-55: Exposed crack surface for Dent F, Specimen **7.**

As shown in Fig. 3-56, similar type periphery cracking developed as in the case with the backhoe tooth dent oriented in the longitudinal direction.

Figure 3-56: Periphery cracking at transverse backhoe tooth dent (Type BH-T), Dent E, Specimen 3

3.9.6 Fatigue Behavior of Rock Dents (Type R)

Restrained rocks have induced two types of fatigue cracks. Peripheral cracks developed similar to both Type BH dents and the restrained Type A dents. Some cracks developed in the trough of the dent, none of which initiated on the outside surface of the pipe. The fatigue failures for dent Type R are given in Fig. 3-57. Several of the rocks broke during testing. They usually maintained their shape due to confinement inside the dent after breaking. Figure 3-58 shows a rock that kept its *shape* until the restraint force was removed. This took away the compressive confinement allowing it to fall apart. Rocks can break, but they still *can* apply restraining forces due to the confinement. Contact deformation caused by a rock is shown on Fig. 3-59. The deformation does not create any cracks since the area is in compression under a restrained rock.

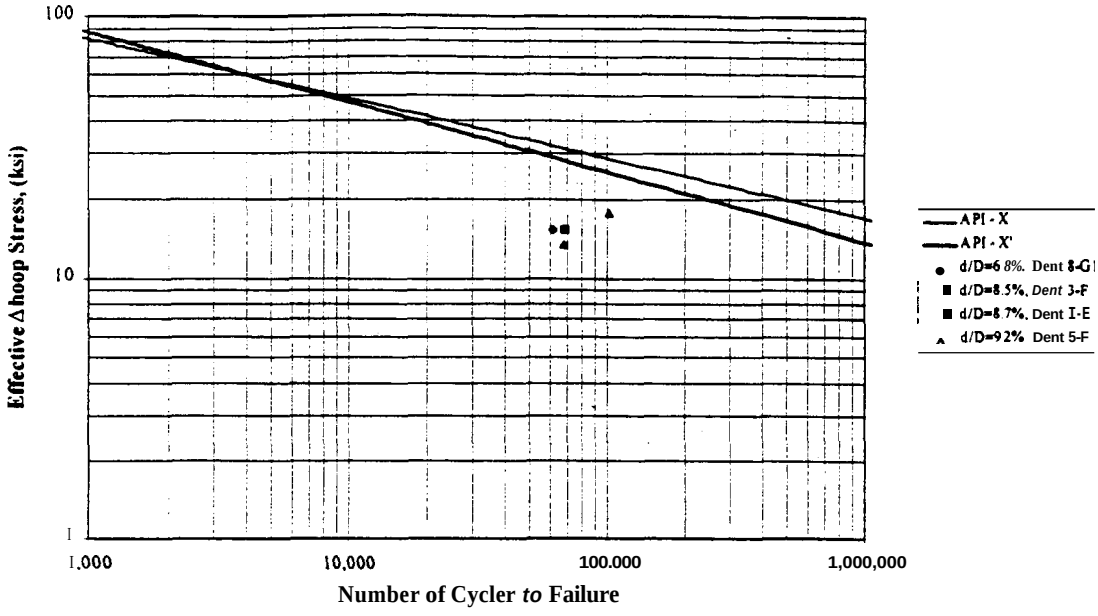

Figure 3-57: S-N plot of fatigue failures for Type R dents.

Figure 3-58: Fractured rock after completion of fatigue testing, Dent H, Specimen 8.

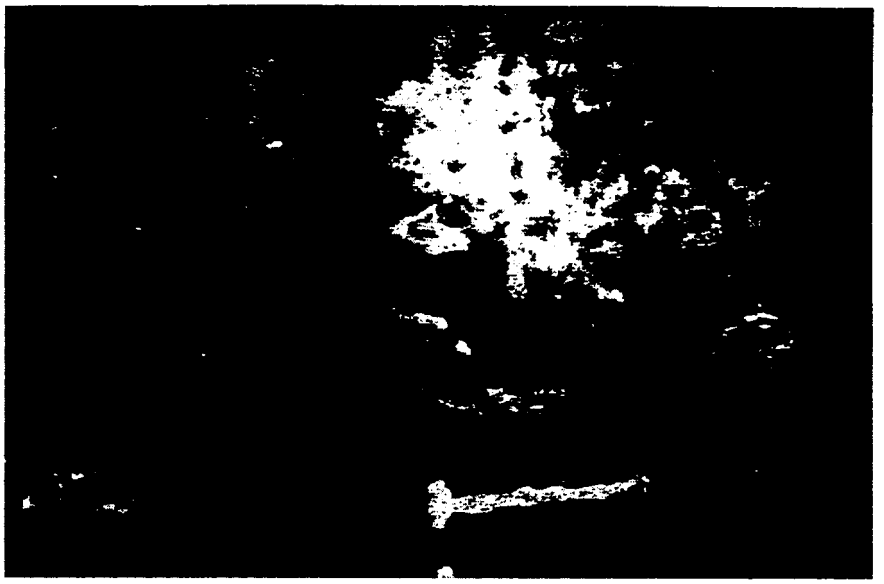

Figure 3-59: View of rock contact deformation, Dent F, Specimen 8.

Two of the four Type R failures were from peripheral leaks. An example of a Type R peripheral crack is given in Fig. 3-60. This failure occurred after a static proof test after cycling was completed. These two dents have initial d/D ratios of 12.5 percent and 15 percent. The fatigue lives of these failures are similar to type BH failures of similar initial d/D.

The other two failures initiated in the trough of the dent. Both cracks initiated on the inside surface of the pipe. Each failure tripped the low limit switch of the hydraulic controller. With pressurization, water leaked from under the restrained rocks at low pressure. After restraint removal, high pressurization yielded no leaks for both dents. With no pressure, the internal surface under the restrained rock has a high residual tensile stress. With pressure, the dent wants to rebound which reduces the tensile stresses on the internal surface and closes the fatigue crack. Cycling at low pressures is the worst case for this failure type. This type of fatigue crack is not noticeable by visual inspection or by pressurization which makes a crack of this type difficult to detect.

Figure 3-60: View of Dent F, Specimen 8 showing rock and leaking fatigue crack at the outer periphery (right side) of the dent.

3.9.7 Yield Stress Determination

The yield strength was determined for each of the pipe specimens. After cyclic testing was completed, sections were cut out from which tension test specimens were machined. The dimensions of the tension specimens are given in Fig. 3-61. The specimens were oriented to determine the pipe transverse yield strength. Each specimen was flattened without heating. An MTS hydraulic testing machine was used with an extensometer with a gage length of 1.5 in.

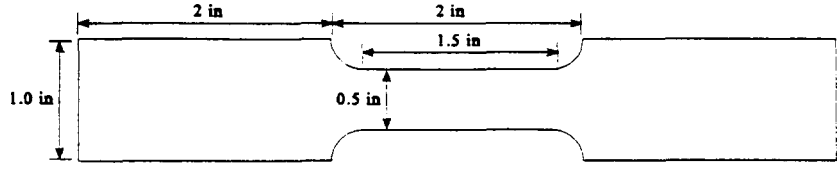

Figure 3-61: Tension Test Specimen.

Two methods were used to determine the yield strength. The yield was first determined using API Specification 5L. The yield is determined to be the stress value at a corresponding strain of 0.5 percent. For a comparison, the 0.2 percent offset method was also used to determine the yield strength. In this method, a line is drawn parallel to the elastic part of the stress-strain curve with a strain offset of 0.2 percent. The yield is equal to the stress at the intersection of the line and curve. The yield strengths for the pipe specimens are given in Table 3-5. Both methods give similar results for all specimens. The stress versus strain curve for each tension specimen is plotted in Fig. 3-62.

Table 3-5: Yield strengths for pipe specimens using both 0.2% and API 5L methods of determination.

		Yield Strength, (ksi)	
		0.2% Offset	API 5L
Specimen	Grade	Method	0.5%
1, 2	X60	75	76
3	X42	54	55
4	X60	62	63
5	X42	49	51
6	X42	53	55
7, 8	X60	64	65
9, 10, 11	X60	69	69
12, 13	B (35 ksi)	51	52
14, 15	B (35 ksi)	29	29

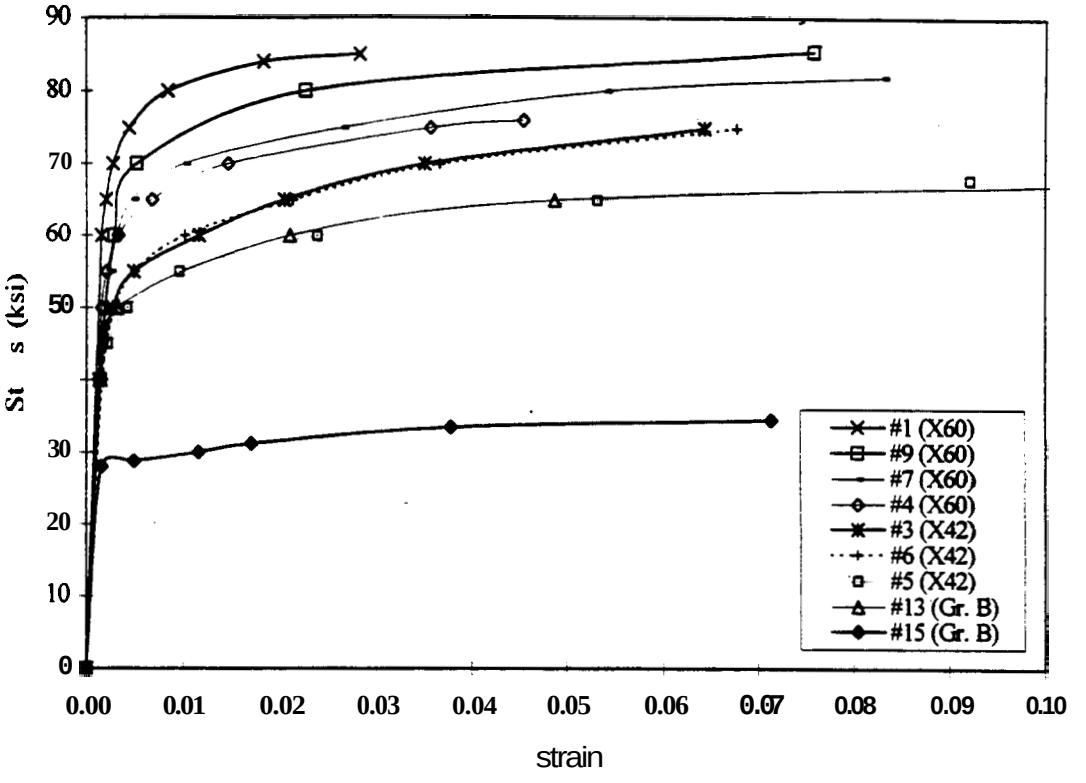

Figure 3-62: Stress versus strain curves for pipe tension specimens.

3.9.8 Effect of Straps on Hoop Stress

The purpose of the straps is to restrain a dent. Each strap makes a loop around the pipe cross section. This can allow the straps to carry some of the hoop stress associated with pressure. Five strain gages were placed on Specimen 9 to compare hoop strains near restrained dents with other areas of the pipe. The location of the gages is given in Fig. 3-63. The gages were placed 120 degrees away from the dents. Six straps were used to restrain the dent. Gages A, B, and C were placed between straps. Gage D was placed between dents. Gage E was placed under an unrestrained dent.

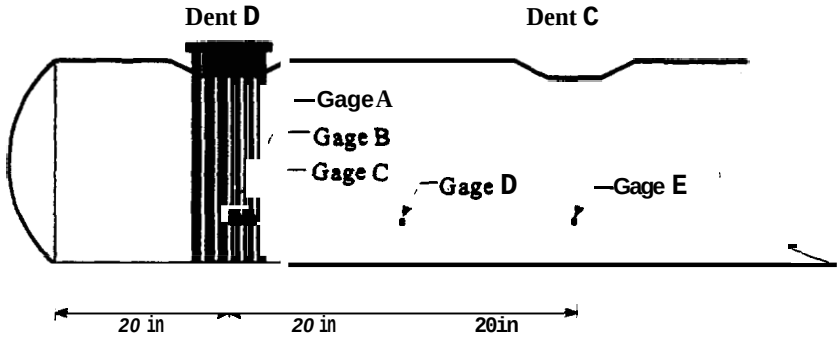

Figure 3-63: Strain gage locations for Specimen 9.

Strain data was collected at several different pressures for each gage. The gages were placed on the pipe after initial pressurization. Thus, the data represents the change in hoop strain after dent rebound due to pressurization: The data is given in Table 3-6.

Table 3-6: Strain measures for Specimen 9.

Pressure	Measured Hoop Microstrains				
(psi)	A	B	C	D	E
100	98	96	94	100	85
200	224	218	217	224	202
300	338	342	328	351	324
400	448	455	450	476	451
500	575	575	576	604	580
600	696	706	700	735	707
626	726	732	724	758	732

The data for all the gages is comparable. Thus, the hoop stress is not affected by the straps of a restrained dent. The strains of the gages under restrained and unrestrained dents are similar. The gage between the dents has slightly higher values. The similarity of the data is given in Figure 3-64. The top line represents the equivalent strain of the pipe based on Hooke's

Law. The difference between the theoretical and measured values **may** be caused by the geometry of the dented **pipe.**

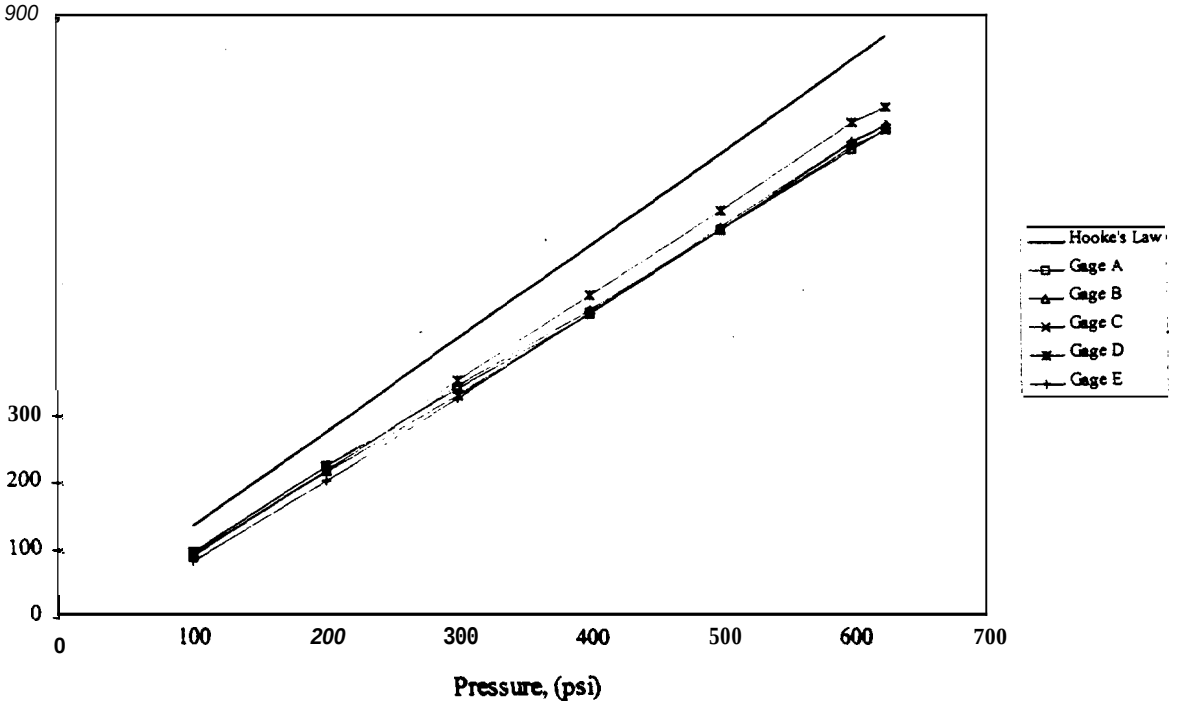

Figure 3-64: Strain versus **pressure for** Specimen 9.